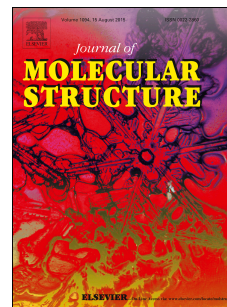


Accepted Manuscript

Polymorphs and solvatomorphs of azilsartan medoxomil: Elucidation of solvent-induced construction and conformational diversity

Xian-Rui Zhang, Sai-Fei He, Shuo Zhang, Jing Li, Shan Li, Jin-Song Liu, Lei Zhang



PII: S0022-2860(16)31063-8

DOI: [10.1016/j.molstruc.2016.10.022](https://doi.org/10.1016/j.molstruc.2016.10.022)

Reference: MOLSTR 23023

To appear in: *Journal of Molecular Structure*

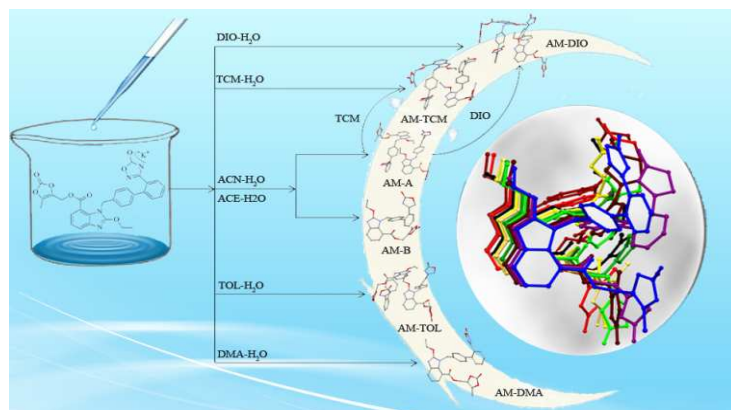
Received Date: 28 March 2016

Revised Date: 4 October 2016

Accepted Date: 6 October 2016

Please cite this article as: X.-R. Zhang, S.-F. He, S. Zhang, J. Li, S. Li, J.-S. Liu, L. Zhang, Polymorphs and solvatomorphs of azilsartan medoxomil: Elucidation of solvent-induced construction and conformational diversity, *Journal of Molecular Structure* (2016), doi: 10.1016/j.molstruc.2016.10.022.

This is a PDF file of an unedited manuscript that has been accepted for publication. As a service to our customers we are providing this early version of the manuscript. The manuscript will undergo copyediting, typesetting, and review of the resulting proof before it is published in its final form. Please note that during the production process errors may be discovered which could affect the content, and all legal disclaimers that apply to the journal pertain.



ACCEPTED MANUSCRIPT

Polymorphs and solvatomorphs of azilsartan medoxomil: Elucidation of solvent-induced construction and conformational diversity

Xian-Rui Zhang^a, Sai-Fei He^a, Shuo Zhang^a, Jing Li^a, Shan Li^{a,*}, Jin-Song Liu^b, Lei Zhang^{a,*}

^a *School of Bioscience and Bioengineering, South China University of Technology, Guangzhou 510006, P. R.*

China

^b *Guangzhou Institutes of Biomedicine and Health, Chinese Academy of Sciences, Guangzhou 510530, P. R.*

China

* Corresponding author.

E-Mail address: lishan@scut.edu.cn (S. Li); lzhangce@scut.edu.cn (L. Zhang).

ABSTRACT:

Two polymorphs (AM-A and AM-B) of azilsartan medoxomil (AM) and four AM solvatomorphs with toluene (AM-TOL), 1,4-dioxane (AM-DIO), chloroform (AM-TCM) and N,N-dimethylacetamide (AM-DMA) have been prepared by the hydrolysis of azilsartan medoxomil potassium in aqueous-organic solutions. In the crystal structures of two polymorphs and three solvatomorphs (AM-TOL, AM-DIO and AM-TCM), two asymmetric AM molecules form the dimeric cycle-like structures via intermolecular N–H···N hydrogen bonds in $R_2^2(26)$ ring, while AM-DMA shows intermolecular N–H···O hydrogen bond between AM and DMA molecules. The hydrogen bonds (C–H···O or C–H···N) and π ··· π (or C–H··· π) interactions are helpful to stabilize the conformational diversity of AM. The solvent-induced experiment shows that solvent molecules have great influence on the solvatomorph formation and DIO can form the most steady solvatomorph than other solvents. The thermal study demonstrates that toluene molecules in three solvatomorphs (AM-TOL, AM-DIO and AM-TCM) are the most difficult to remove from the cage. Our results illustrate that the solvent plays significant role in tuning the size of the cage and producing the conformational diversity of AM molecules.

Keywords: Azilsartan medoxomil; Polymorph; Solvatomorph; Crystal structure; Hydrogen bond

1. Introduction

Polymorphs and solvatomorphs have been the important issues in chemical and pharmaceutical industries [1-5]. Especially in pharmaceutical industry, polymorphs of active pharmaceutical ingredients (APIs), although identical in chemical composition, have received many concerns for half a century due to the differences in solubility, dissolution rate, bioavailability, filterability, physical stability and other properties [6-11]. For the conformational polymorphs of APIs, the conformers sometimes cannot interconvert randomly due to the distinct potential energy between the conformers, which may cause the different affinity to enzyme or targets and further affect the pharmacology [2, 12-16]. Also, solvatomorph has been a subject of intense interest in order to control some polymorph formation and drying process in the manufacture of APIs [17-20].

Azilsartan medoxomil (AM) and azilsartan medoxomil potassium (AMP, **Scheme 1.**) are regarded as the prodrug of azilsartan (Az), which are widely used in the treatment of circulatory diseases such as hypertension, cardiac diseases, nephritis, stroke and some other cardiovascular diseases [21-24]. As angiotensin receptor blocker, azilsartan should interact catalytically with the important residues of angiotensin II receptor type 1 (AT_1) through the active moieties. Therefore, the right conformer of azilsartan could bind tightly to AT_1 to feature high bioactivity [25-27]. In the molecular structures of AM, the biphenyl rings could not freely rotate to accommodate the substrate-binding pocket due to the strong conjugate action, which maybe produces many different molecular configurations. In the present work, the solvate-assisted molecular assemblies are performed in details to explore the molecular conformations of AM by hydrolyzing AMP under aqueous-organic mixtures. Two AM polymorphs (AM-A, AM-B) and four solvatomorphs with toluene (AM-TOL), 1,4-dioxane (AM-DIO), chloroform (AM-TCM) and *N,N*-dimethylacetamide (AM-DMA) have been prepared and well characterized by physical methods

2. Experimental

2.1. Instrumentations and materials

All solvents and reagents (analytical grade) were obtained commercially and used as received unless otherwise mentioned. Nuclear magnetic resonance ($^1\text{H-NMR}$) spectra were recorded on the 400 MHz instrument (Bruker, Germany) using $\text{DMSO-}d_6$ (Aldrich) as solvent and tetramethylsilicane as an internal standard. Thermogravimetric and differential scanning calorimetry (TG-DSC) experiments were carried out in Netzsch STA449C equipment (Netzsch, Germany) with the heating rate of $5^\circ\text{C}/\text{min}$ under a nitrogen gas purge with a flow of $20\text{ mL}/\text{min}$. Fourier infrared (FT-IR) spectra were performed on a Bruker Vector 33 in the $4000\text{-}400\text{ cm}^{-1}$ range. Powder X-ray diffraction (PXRD) patterns were obtained with a D8 ADVANCE powder diffractometer (Bruker, Germany) coupled with a $\text{Cu K}\alpha$ radiation tube ($\lambda = 1.5418\text{ \AA}$, $V = 40\text{ kV}$ and $I = 40\text{ mA}$) and 2θ scan in the $3\text{-}60^\circ$ range. Data were further processed using the JADE software (Rigaku, Japan). The simulated XRPD patterns were calculated using the MERCURY software (version 3.5.1; Cambridge Crystallographic Data Center, Cambridge, UK). Crystal morphologies were analyzed by Olympus BX41 microscope (Tokyo, Japan).

2.2. Preparation of polymorphs and solvatomorphs

2.2.1. Preparation of polymorph AM-A.

AMP (40 mg) was dissolved in 14 mL of acetonitrile/water (6:1, v/v) or acetone/water (6:1, v/v), and stirred at $50\text{-}55^\circ\text{C}$ for 2 h. The resulting solution was slowly cooled down to room temperature for slow evaporation. The fine sheet crystals suitable for single crystal X-ray diffraction were obtained after 7 days. Yield: 22 mg (55%). $^1\text{H-NMR}$ δ (ppm): 12.36 (bs, 1H), 7.74 (d, $J = 7.8\text{ Hz}$, 1H), 7.68-7.63 (m, 2H), 7.56-7.51 (m, 2H), 7.47 (d, $J = 7.6\text{ Hz}$, 1H), 7.23-7.19 (m, 3H), 7.00 (d, $J = 7.8\text{ Hz}$, 2H), 5.55 (s, 2H), 5.11 (s, 2H), 4.60 (q, $J = 7.0\text{ Hz}$, 2H), 2.16 (s, 3H), 1.39 (t, $J = 7.0\text{ Hz}$, 3H). The result is in good accordance with the literatures [28-29].

2.2.2. Preparation of polymorph AM-B.

AM-B was obtained unexpectedly during the crystallization process of AM-A in acetonitrile/water (6:1, v/v) system. During the repeated experiment for polymorph AM-A, a small needle crystal was found attaching to the beaker along the surface of solution. The colorless crystal was identified to be suitable for single crystal X-ray diffraction. We also attempted to repeat the crystallization conditions for AM-B, but failed.

2.2.3. Preparation of solvatomorph AM-TOL

AM-TOL was obtained by dissolving AMP (20 mg) in 14 mL of the TOL/water (6:1, v/v) mixture under 50-55°C for 3 h, and the resulting solution was slowly cooled down to room temperature. The aqueous layer was removed and the organic layer was left for slow evaporation. The fine block crystals suitable for single crystal X-ray diffraction were obtained after 20 days. Yield: 12 mg (60%). ¹H-NMR δ (ppm): 12.37 (bs, 1H), 7.73 (d, J = 7.7 Hz, 1H), 7.68-7.63 (m, 2H), 7.56-7.51 (m, 2H), 7.47 (d, J = 7.6 Hz, 1H), 7.27-7.12 (m, 5.5H), 7.00 (d, J = 7.9 Hz, 2H), 5.55 (s, 2H), 5.11 (s, 2H), 4.60 (q, J = 7.0 Hz, 2H), 2.30 (s, 1.5H), 2.16 (s, 3H), 1.38 (t, J = 7.0 Hz, 3H).

2.2.4. Preparation of solvatomorph AM-DIO

The same procedure as that of AM-TOL was applied with DIO/water (1:1, v/v) mixture in place of TOL/water one to obtain crystals in 10 days in 77% yield. ¹H-NMR δ : 12.37 (bs, 1H), 7.73 (d, J = 7.9 Hz, 1H), 7.68-7.64 (m, 2H), 7.56-7.52 (m, 2H), 7.47 (d, J = 7.5 Hz, 1H), 7.23-7.19 (m, 3H), 7.00 (d, J = 7.7 Hz, 2H), 5.56 (s, 2H), 5.12 (s, 2H), 4.60 (q, J = 7.0 Hz, 2H), 3.57 (s, 6H), 2.16 (s, 3H), 1.39 (t, J = 7.0 Hz, 3H).

2.2.5. Preparation of solvatomorph AM-TCM

AM-TCM was obtained analogously with AM-TOL, but the single crystals were obtained by dissolving AM-A (20 mg) in chloroform (8 mL). The resulting solution was left for slow evaporation. Yield: 17 mg (85%). ¹H-NMR δ : 12.40 (bs, 1H), 8.32 (s, 1H), 7.73 (d, J = 7.8 Hz, 1H), 7.69-7.63 (m, 2H), 7.56-7.51 (m, 2H), 7.46 (d, J = 7.6 Hz, 1H), 7.23-7.18 (m, 3H), 6.99 (d, J = 8.0 Hz, 2H), 5.55 (s, 2H), 5.12 (s, 2H), 4.60 (q, J = 6.9 Hz, 2H), 2.16 (s, 3H), 1.39 (t, J = 7.0 Hz, 3H).

2.2.6. Preparation of solvatomorph AM-DMA

AM-DMA was obtained by dissolving AMP (40 mg) in 6 mL of DMA/water (1:1, v/v) solution and leaving the solution for slow evaporation at room temperature. The fine block crystals suitable for single crystal X-ray diffraction were obtained after 7 days. Yield: 18 mg (45%). $^1\text{H-NMR}$ δ : 12.36 (bs, 1H), 7.73 (d, $J = 7.8$ Hz, 1H), 7.68-7.63 (m, 2H), 7.56-7.51 (m, 2H), 7.47 (d, $J = 7.5$ Hz, 1H), 7.23-7.19 (m, 3H), 7.00 (d, $J = 7.7$ Hz, 2H), 5.55 (s, 2H), 5.11 (s, 2H), 4.60 (q, $J = 6.9$ Hz, 2H), 2.94 (s, 3H), 2.78 (s, 3H), 2.16 (s, 3H), 1.95 (s, 3H), 1.38 (t, $J = 7.0$ Hz, 3H).

2.3. Solvent-induced study

In order to investigate the solvent effect on the formation of solvatomorphs, solvent-induced study was carried out by complexing AM-A (1000 mg) with the mixed solvent composed of the equimolar amount of TOL, acetone (ACE), acetonitrile (ACN), DIO, TCM and dichloromethane (DCM) (a total volume of about 18 mL) as solvent molecules. The suspension mixture was stirred at room temperature, and then about 0.5 mL suspension mixture was collected into micro centrifuge tubes at 2, 4, 8, 12, 24, 48 and 96 hour time points. Samples were separated by centrifuging at 12,000 rpm for 2 min, and then the solid precipitates were washed quickly with diethyl ether for twice (0.5 mL). The final solids were dissolved in $\text{DMSO-}d_6$ for $^1\text{H-NMR}$ analyses. The mixture was left for three months at room temperature, and the resulting solid was checked again according to the methods above.

2.4. X-ray crystallography

All the crystal structures were determined by the single-crystal X-ray diffraction experiments. The diffraction data for AM-B and AM-TOL crystals were collected on an Oxford Xcalibur Gemini Ultra diffractometer with an Atlas detector operating at 40 kV and 40 mA using Cu $K\alpha$ radiation ($\lambda = 1.54178 \text{ \AA}$), while the other diffraction data for AM-A, AM-DIO, AM-TCM and AM-DMA were performed on a Bruker Apex II CCD diffractometer

operating at 50 kV and 30 mA using Mo K α radiation ($\lambda = 0.71073 \text{ \AA}$). All the crystal structures were solved by direct methods using SHELXS program and refined with SHELXL program [30-31]. The final refinements were performed by full-matrix least-squares methods with anisotropic thermal parameters for all non-hydrogen atoms on F^2 . The hydrogen atoms on non-carbon atoms were located from difference Fourier maps and the hydrogen atoms riding on the carbon atoms were determined with theoretical calculation and refined isotropically. Crystallographic parameters and hydrogen bonds were listed in Tables 1 and 2.

3. Result and discussion

3.1. Preparation of polymorphs and solvatomorphs

AMP approved by US FDA as API in Edarbi tablet is unstable and easily hydrolyzed to azilsartan (Az) in the gastrointestinal tract after administration. However, AMP can hydrolyze to produce AM in aqueous-organic systems. Based on the reaction mechanism above, the crystal forms could be prepared by hydrolyzing AMP in the aqueous-organic solvents, respectively. The fine crystals of AM-TCM suitable for single crystal X-ray diffraction could be easily obtained by crystallizing AM-A from TCM as a sole solvate. In this study, the mixed solvents are divided into two categories: whole intersoluble and partial intersoluble dual-liquid systems. The microscopic images for all six compounds show different morphologies as shown in Fig. 1. The solvent amounts in four solvatomorphs are also determined by $^1\text{H-NMR}$ spectra and TG analyses, which are excellent strategies to identify the amount of disordered solvent molecules. The $^1\text{H-NMR}$ results shown in Fig. 2 suggest being 0.51, 0.75, 1.00 and 1.00 solvent molecules per AM molecule in AM-TOL, AM-DIO, AM-TCM and AM-DMA (Figs. S1-S5 in Supporting Information), respectively, which are in good agreement with the corresponding results of single crystal X-ray diffraction analyses and TG analyses. The IR spectra (Fig. S6 in Supporting Information) feature some apparent differences in vibration peaks (intensity and shape) observed in the ranges of 1750-1500 and 1100-700 cm^{-1} suggesting the change in the vibration modes of AM molecules when the solvates are formed.

3.2. Crystal structure analyses

Polymorph AM-A is in the solvent-free form crystallized in monoclinic $P2_1/n$ space group. Two asymmetric AM conformers coexist in the unit cell as shown in Fig. 3a. In the crystal structure, the N–H \cdots N hydrogen bonds between oxadiazole moiety and benzimidazole group are the major interaction connecting the two asymmetric AM conformers to form a dimeric cycle-like structure within the $R_2^2(26)$ hydrogen bond (Fig. 3a). The H \cdots N distances in N–H \cdots N hydrogen bonds are determined as 1.90 Å and 1.96 Å, respectively (Table 2). Importantly, two dimeric unit are further connected through an offset $\pi\cdots\pi$ stacking interactions (Fig. 3a). Furthermore, the dimeric units associate along the *ac*-plane through C–H $\cdots\pi$ interactions to form one-dimensional structure (Table 3). In the crystal structure, two phenyl rings (C and D) and an oxadiazoles ring don't lie in the same plane, and the dihedral angles between C and D rings are 44.2(2) and 47.3(2)°, respectively (Table 4), which suggests that the energy stabilized by the π -electrons delocalization of two phenyl rings is perturbed by the steric hindrance. It is found out that the biphenyl and dioxolyl groups are located on different sides of the benzimidazolyl plane in one conformer, and on the same side in the other conformer. The weak C–H \cdots N and C–H \cdots O hydrogen bonds not only connect the dimeric structure, but construct the three-dimensional structure as well (Table 3).

Polymorph AM-B is also solvent-free form crystallized in monoclinic $C2/c$ space group, and only one AM conformer exists in the asymmetric unit as shown in Fig. 3b. The dimer is also cyclized through intermolecular $R_2^2(26)$ N–H \cdots N hydrogen bonds as found in AM-A, while the dimeric cycle-like units extend through $\pi\cdots\pi$ stacking interactions along the *c*-axis to form one-dimensional chain structure (Fig. 3b, Table 3). The biphenyl group and the dioxolyl ring are located on the same side of the benzimidazolyl group in the conformer. The two phenyl rings are not in the same plane and form the dihedral of 51.5(2)° to meet the direction of the hydrogen bond. Additionally, the dimeric skeleton is stabilized by intermolecular C–H $\cdots\pi$ interactions in the dimeric structures (Table 3). Although the dimeric units are automatically oriented in angular shape to each other, the solvent accessible void is

found to be 166 \AA^3 in the crystal lattice obtained using the PLATON [32]. The weak C–H \cdots N and C–H \cdots O hydrogen bonds is only found between the dimers to construct the three-dimensional structure (Table 3).

Solvatomorph AM–TOL crystallizes in triclinic P-1 space group. Two asymmetric AM conformers coexist in the unit cell as shown in Fig. 4a. As found in AM-A and depicted in the Fig. 3, two asymmetric AM molecules are connected by $R_2^2(26)$ hydrogen bonds consisting of oxadiazole and benzimidazole groups to form the dimeric cycle-like structure. The H \cdots N distances in N–H \cdots N hydrogen bonds are determined to be 2.01 \AA and 2.00 \AA , respectively (Table 2). In the crystal structure, the biphenyl group and the dioxolyl ring are located on the same side of the benzimidazolyl plane in two conformers, which is obviously different from those in AM-A. These conformations are advantageous to form a cage through two dimers, which is occupied by two toluene molecules (Fig. 4a). It is strange to find that only the C–H \cdots N interactions are observed within the dimer, but the C–H $\cdots\pi$ and $\pi\cdots\pi$ stacking interactions are eliminated, which is totally different from polymorphs AM-A and AM-B.

In the solvatomorph AM-DIO, two asymmetric AM conformers coexist in the unit cell to form the dimer connected by $R_2^2(26)$ N–H \cdots N hydrogen bond (Fig. 4b), which is consistent with AM-TOL. The biphenyl group and the dioxolyl ring in the crystal structure are located on the same side of the benzimidazolyl plane in one conformer, while in the other conformer, The biphenyl group keeps locating on one side, and the dioxolyl ring is nearly lying in the same plane with benzimidazolyl ring, which is obviously different from those found in AM-TOL. The change enables three DIO molecules to be partially wrapped by two dimers, in which the DIO molecules are tightly tied by the C–H \cdots O hydrogen bonds between AM and DIO molecules (C–H \cdots O angles being 164 and 172° , C \cdots O distances being $3.455(3)$ and $3.516(4) \text{ \AA}$, respectively) (Fig. 4b).

The crystal structure of AM-TCM is very similar to AM-TOL, and two asymmetric AM molecules are connected by two hydrogen bonds consisting of oxadiazole and benzimidazole groups to form the cycle-like structure. Four chloroform molecules are encapsulated in the cage formed by two dimers (Fig. 4c).

Solvatomorph AM-DMA crystallizes in a monoclinic $P2_1/n$ space group, and only one AM conformer exists in the unit cell. AM molecule forms hydrogen bond with the carbonyl O atom of DMA molecule as receptor as shown in Fig. 5. The biphenyl group and the dioxolyl ring are located on the same side of the benzimidazolyl plane in the conformer. The intermolecular N–H \cdots O hydrogen bond mode is obviously different from the polymorphs and the other solvatomorphs which are N–H \cdots N mode composed of benzimidazolyl and oxadiazolyl groups. The weaker intermolecular C–H \cdots O hydrogen bonds form $R_2^2(24)$ and $R_2^2(38)$ rings as shown in Fig. 5, and further expand to construct three-dimensional structure (Table 3).

3.3. PXRD analyses

Powder X-ray diffraction is an effective tool to differentiate polymorphs and/or solvatomorphs based on line profile. The PXRD patterns for AMP, AM-A and four solvatomorphs are shown in Fig. 6. The base lines of the experimental patterns are nearly flat and the peaks are symmetric and sharp suggesting that the samples have excellent crystallinity. Calculated PXRD patterns are generated from the single crystal structures using Mercury software. The experimental PXRD patterns are affected by preferred orientation effects and match well with the calculated patterns in 2θ , which indicates that the crystal structures are representative for the bulk materials.

3.4. Solvent-induced study

The solvent-induced results are shown in Fig. 7 and suggest that CH_3CN can combine with AM molecules quickly, TCM and DCM molecules can gradually insert into AM-A molecule up to 0.36 and 0.24 molecules per AM molecule after 24 h soaking. DIO can slowly insert into AM-A in the experimental time, but toluene has hardly been detected. Keeping the suspension undisturbed for three months at room temperature, the solid gradually and wholly transforms to be crystal form, which is identified to be AM-DIO by $^1\text{H-NMR}$ and single crystal X-ray diffraction (unit cell parameters: $a = 12.473(3) \text{ \AA}$, $b = 14.823(3) \text{ \AA}$, $c = 18.437(4) \text{ \AA}$, $\alpha = 94.552(4)^\circ$, $\beta = 108.627(4)^\circ$, $\gamma = 99.373(4)^\circ$, $V = 3155.3(12) \text{ \AA}^3$). This phenomenon suggests that AM-A without accessible

void could change its stereo configuration to form the cage with the help of CH₃CN (TCM or DCM) solvent and that DIO has been preponderant in the competitive inclusion into the void. Toluene can hardly into the cage caused by the dimeric AM molecules. From these facts combined with the crystal structures, it is found that the solvents may freely insert/escape from the void formed by two dimeric units, and then AM gradually transforms into the stable state AM-A when the organic solvents (acetonitrile or acetone) are small molecules in volume without forming the hydrogen bond between solvent and AM molecules, When the solvents (toluene or chloroform) are slightly larger molecules and do not form hydrogen bond with AM molecules, the solvents are encapsulated into the cage constructed by two dimers. When the DIO solvent form the weak hydrogen bond with AM molecules, the cage with two holes are formed to be filled with three DIO molecules in two dimers. However, the solvent DMA completely breaks the dimeric cage through its hydrogen bond to AM molecule. During the transformation process, the conformational flexibility is very important to match the requirement of configuration through the different conformers and to reduce the steric hindrance. Ten different conformers produced by solvent-induced effect in six compounds are found owing to the significantly conformational flexibility (Fig. 8), and the dihedral angles between A-C, C-D and D-E are in the ranges of 73.4(3) -89.7(3)°, 40.5(2)-51.5(2)° and 49.3(2)-62.5(3)° as listed in Table 4, respectively. The compounds except AM-A show the existence of solvent-accessible voids. The solvent amounts must match the requirement of the void volumes (The approximate volumes for the organic solvent molecules are 86 Å³ for acetonitrile, 122 Å³ for acetone, 132 Å³ for TCM, 142 Å³ for DIO, 155 Å³ for DMA, 176 Å³ for TOL), and the calculated void volumes after removal of solvent molecules based on the crystal data follow the order: AM-TCM (541 Å³) > AM-DIO (508 Å³) > AM-TOL (486 Å³) > AM-DMA (318 Å³) > AM-B (166 Å³).

Hydrogen bond also plays dominant role in controlling molecular assemblies and stabilizing the spatial configurations of AM molecules due to its sufficient directionality [33-42]. In the crystal structures of polymorphs

(AM-A and AM-B), the hydrogen bond interactions result in the different molecular conformers and crystal symmetry. For three solvatomorphs (AM-TOL, AM-DIO and AM-TCM), the N–H···N hydrogen bonds are unique formed by benzimidazolyl and oxadiazolyl groups in R₂²(26) ring. The H···N distances and N–H···N angles are in the ranges of 1.88-2.06 Å and 170-176°, which feature the stronger hydrogen bond interactions with high linearity in assemble the molecular structures. Furthermore, the non-classical hydrogen bond interactions (C–H···N or C–H···O) are also found in all compounds, which further strengthen the crystal structures and regulate the bioactivity [36-41]. Another important factor on molecular assembly is C–H··· π interactions and π ··· π interactions (Table 3) [42-45], which are the dispersion interaction between AM molecules. Although these weak interactions are unable to control the molecular orientation in molecular assemblies, they actually impact the stability and the crystal packing.

3.5. Thermal stability analysis

Polymorph AM-A and four solvatomorphs are investigated by TG-DSC under nitrogen gas atmosphere (Figs. S7-S11 in Supporting Information). The TGA profiles shown in Fig. 9 feature that AM-A has no weight loss before decomposition at 217 °C, suggesting that AM-A sample does not contain solvent molecules. AM-TOL shows obvious mass loss in the 140-205 °C temperature range, and loses about 7.15% of total molecular weight corresponding to half a TOL molecule per AM molecule (theoretical value: 7.50%). AM-DIO exhibits apparent mass loss in the temperature range of 120-200 °C, and loses about 10.05% of total molecular weight corresponding to three-quarters DIO molecule per AM molecule (theoretical value: 10.41%). AM-TCM shows obvious mass loss in the temperature range of 100-213°C, and loses about 17.14% of total molecular weight corresponding to one TCM molecule per AM molecule (theoretical value: 17.35%). AM-DMA shows mass loss in the temperature range of 125-220 °C, and loses about 12.86% of total molecular weight corresponding to one DMA molecule per AM molecule (theoretical value: 13.29 %). These results on TG analyses further identifies the conclusions of ¹H-NMR

spectra and single crystal X-ray diffractions.

3.6. Hirshfeld surface analysis

Molecular Hirshfeld surfaces calculations were performed by CrystalExplorer 3.1 software based on results of single crystal X-ray diffraction studies [46-48], which can be used to identify the nature and type of the intermolecular interactions, and proportion of the interaction in the crystal. Strengths of intermolecular interactions and a 2-D fingerprint plot (Fig. S12 in Supporting Information) within the crystal are mapped onto the Hirshfeld surfaces using the descriptor d_{norm} , which is a ratio encompassing the distance of any surface point to the nearest interior (d_i) and exterior (d_e) atom to the van der Waals radii of the atoms. Percentage distribution of various intermolecular contacts to the Hirshfeld surface areas of ten AM conformers have been shown in Fig. 10. Overall, the majority of Hirshfeld surface contribution is H...H, H...O, H...C and H...N close contacts. The H...H, H...O, H...C and H...N contacts vary from 25.0%, 21.5%, 14.7% and 6.6% to 42%, 34.2%, 21.2% and 8.8% for ten conformers, respectively. Due to the typical C-H...O interactions and/or classical N-H...O interactions in AM-A, AM-DIO and AM-DMA, the H...O interactions in AM-A, AM-DIO and AM-DMA have a more significant increase in percentage distribution than those in AM-B, AM-TOL and AM-TCM. For two conformers of AM-TCM, other contacts contribute 20.6% and 27.7% of the total Hirshfeld surfaces, which are mainly due to extra H...Cl, C...Cl and O...Cl interactions.

4. Conclusion

The solvent-induced conformational assemblies have been illustrated for AM molecules in aqueous-organic systems characterized by a series of physical methods. Six single crystal structures of AM are firstly revealed and ten conformers are found in the studied systems. The solvent can induce the change of AM molecular configurations to form the cage occupied by the solvent molecules *via* intermolecular N-H...N hydrogen bonds. The solvent amount encapsulated in the cage is firmly related to the solvent molecular volume. The non-classical

hydrogen bonds (C–H···N or C–H···O) and the $\pi\cdots\pi$ (or C–H··· π) stacking interactions are observed in the compounds to stabilize the crystal structures and AM molecular configurations.

Acknowledgments

The authors thank Guangdong Provincial Department of Science and Technology (Grant No.: 2012A080800002) and the Fundamental Research Funds of the Central Universities (D215197w) for financial support of this research.

Appendix A. Supporting Information

CCDC 1425965 for AM-B, 1425966 for AM-DIO, 1425967 for AM-DMA, 1425968 for AM-TCM, 1425969 for AM-TOL and 1428179 for AM-A contain the supplementary crystallographic data for this paper. ¹H-NMR spectra, FT-IR, TGA-DSC, 2-D fingerprint plots and crystal data can be found at <http://dx.doi.org/10.1016/j.molstruc>.

References

- [1] H.G. Brittain, *J. Pharm. Sci.* 101 (2012) 464-484.
- [2] H.G. Brittain, *Polymorphism in pharmaceutical solids*, 2nd ed., Informa Healthcare Press, New York, 2009, pp 120-124.
- [3] A.Y. Lee, D. Erdemir, A.S. Myerson, *Ann. Rev. Chem. Biomol. Eng.* 2 (2011) 259-280.
- [4] B. Moulton, M.J. Zaworotko, *Chem. Rev.* 101 (2001) 1629-1658.
- [5] J. Bernstein, *Cryst. Growth Des.* 11 (2011) 632-650.
- [6] M. Pudipeddi, A. Serajuddin, *J. Pharm. Sci.* 94 (2005) 929-939.
- [7] A.A. Ali, A. Farouk, *Int. J. Pharm.* 9 (1981) 239-243.
- [8] C. Herman, B. Haut, V. Halloin, V. Vermeylen, T. Leyssens, *Org. Process Res. Dev.* 15 (2011) 774-782.
- [9] L.F. Huang, W.Q. Tong, *Adv. Drug Delivery Rev.* 56 (2004) 321-334.
- [10] B. Rodríguez-Spong, C.P. Price, A. Jayasankar, A.J. Matzger, N.R. Rodríguez-Hornedo, *Adv. Drug Delivery Rev.* 56 (2004) 241-274.
- [11] X.C. Yang, A.S. Myerson, *CrystEngComm* 17 (2015) 723-728.
- [12] A.J. Cruz-Cabeza, J. Bernstein, *Chem. Rev.* 114 (2014) 2170-2191.

- [13] A. Nangia, *Acc. Chem. Res.* 41 (2008) 595-604.
- [14] S. SeethaLekshmi, T.N. Guru Row, *Cryst. Growth Des.* 12 (2012) 4283-4289.
- [15] C.P. Price, A.L. Grzesiak, M. Lang, A.J. Matzger, *Cryst. Growth Des.* 2 (2002) 501-503.
- [16] L.Y. Pfund, B.L. Chamberlin, A.J. Matzger, *Cryst. Growth Des.* 15 (2015) 2047-2051.
- [17] A. Llinàs, J.M. Goodman, *Drug Discov. Today* 13 (2008) 198-210.
- [18] Y. Li, L. Li, Y. Zhu, X. Meng, A. Wu, *Cryst. Growth Des.* 9(2009) 4255-4257.
- [19] X. Wang, N. Gong, S. Yang, G. Du, Y. Lu, *J. Pharm. Sci.* 103 (2014) 2696-2703.
- [20] S.F. Alshahateet, M.M. Bhadbhade, R. Bishop, M.L. Scudder, *CrystEngComm.* 17 (2015) 877-888.
- [21] W.L. Baker, W.B. White, *Ann. Pharmacother.* 45 (2011) 1506-1515.
- [22] C.J. French, A.T. Zaman, B.E.J. Sobel, *Cardiovasc. Pharm.* 58 (2011) 143-148.
- [23] K. Zaiken, J.W. Cheng, *Clin. Ther.* 33 (2011) 1577-1589.
- [24] Y. Kohara, K. Kubo, E. Imamiya, T. Wada, Y. Inada, T. Naka, *J. Med. Chem.* 39 (1996) 5228-5235.
- [25] T. Kajiya, C. Ho, J. Wang, R. Vilardi, T.W. Kurtz, *J. Hypertens.* 29 (2011) 2476-2483.
- [26] S.I. Miura, N. Nakao, H. Hanzawa, Y. Matsuo, K. Saku, S.S. Karnik, *Plos One* 8 (2013) e79914.
- [27] G. Berellini, G. Cruciani, R. Mannhold, *J. Med. Chem.* 48 (2005) 4389-4399.
- [28] S. Radl, J. Cerny, J. Stach, Z. Gablikova, *Org. Process Res. Dev.* 17 (2013) 77-86.
- [29] S. Garaga, N.C. Misra, A.V. Raghava Reddy, K.J. Prabahar, C. Takshinamoorthy, P.D. Sanasi, K.R. Babu, *Org. Process Res. Dev.* 19 (2015) 514-519.
- [30] G.M. Sheldrick, SHELXS-97, Program for crystal structure solution, University of Göttingen, Göttingen, Germany 1997.
- [31] G.M. Sheldrick, SHELXL-97, Program for crystal structure refinement, University of Göttingen: Göttingen, Germany 1997.
- [32] A.L. Spek, *J. Appl. Crystallogr.* 36 (2003) 36, 7-13.
- [33] G.A. Jeffrey, *An introduction to hydrogen bonding*, Oxford University Press, Oxford, 1997.
- [34] G.K. Such, A.P.R. Johnston, F. Caruso, *Chem. Soc. Rev.* 40 (2011) 19-29.
- [35] R. Taylor, O. Kennard, *Acc. Chem. Res.* 17 (1984) 320-326.
- [36] G.R. Desiraju, *Acc. Chem. Res.* 29 (1996) 441-449.
- [37] J.A. van den Berg, K.R. Seddon, *Cryst. Growth Des.* 3 (2003) 643-661.
- [38] R. Gajda, A. Katrusiak, *Cryst. Growth Des.* 11 (2011) 4768-4774.
- [39] A.B. Baker, C. Samet, *J. Phys. Chem. A* 109 (2005) 8280-8289.

- [40] G.R. Desiraju, T. Steiner, *The weak hydrogen bond in structural chemistry and biology*, Oxford University Press, Oxford, 1999.
- [41] A.C. Pierce, K.L. Sandretto, G.W. Bemis, *Proteins: Struct. Funct. Genet.* 49 (2002) 567-576.
- [42] S. Tsuzuki, A. Fujii, *Phys. Chem. Chem. Phys.* 10 (2008) 2584-2594.
- [43] M. Nishio, Y. Umezawa, J. Fantini, M.S. Weiss, P. Chakrabarti, *Phys. Chem. Chem. Phys.* 16 (2014) 12648-12683.
- [44] J.Y. Wu, H.Y. Hsu, C.C. Chan, Y.S. Wen, C. Tsai, K.L. Lu., *Cryst. Growth Des.* 9 (2014) 258-262.
- [45] J.M. Serrano-Becerra, S. Hernández-Ortega, D. Morales-Morales, J. Valdés-Martínez, *CrystEngComm* 11 (2009) 226-228.
- [46] S.K. Wolff, D.J. Grimwood, J.J. McKinnon, M.J. Turner, D. Jayatilaka, M.A. Spackmann, *CrystalExplorer* 3.1, 2013.
- [47] University of Western Australia, Crawley, Western Australia, 2005–2013. <http://hirshfeldsurface.net/CrystalExplorer>.
- [48] M.A. Spackman, D. Jayatilaka, *CrystEngComm* 11 (2009) 19-32.

Table 1.

Crystallographic parameters of polymorphs and solvates of AM

	AM-A	AM-B	AM-TOL	AM-DIO	AM-TCM	AM-DMA
chemical formula	$C_{30}H_{24}N_4O_8$	$C_{30}H_{24}N_4O_8$	$C_{30}H_{24}N_4O_8$, $1/2C_7H_8$	$C_{30}H_{24}N_4O_8$, $3/4C_4H_8O_2$	$C_{30}H_{24}N_4O_8$, $CHCl_3$	$C_{30}H_{24}N_4O_8$, C_4H_9NO
formula sum	$C_{30}H_{24}N_4O_8$	$C_{30}H_{24}N_4O_8$	$C_{33.5}H_{28}N_4O_8$	$C_{33}H_{30}N_4O_{9.5}$	$C_{31}H_{25}Cl_3N_4O_8$	$C_{34}H_{33}N_5O_9$
formula weight	568.53	568.53	614.60	634.61	686.89	655.65
crystal system	monoclinic	monoclinic	triclinic	triclinic	triclinic	monoclinic
space group	$P2_1/n$	$C2/c$	P-1	P-1	P-1	$P2_1/n$
T [K]	298(2)	298(2)	298(2)	298(2)	298(2)	298(2)
a [Å]	13.867(3)	26.7661(12)	11.8159(3)	12.416(3)	12.171(2)	16.427(5)
b [Å]	13.376(3)	10.7467(5)	13.6418(2)	14.763(3)	13.534(2)	9.562(3)
c [Å]	29.422(6)	20.7113(8)	19.8791(4)	18.392(4)	19.769(3)	21.968(6)
α [°]	90	90	94.115 (1)	94.59(3)	92.250(3)	90
β [°]	99.44(3)	96.097(4)	94.863(2)	108.67(3)	96.380(3)	109.076(4)
γ [°]	90	90	103.192(2)	99.38(3)	102.595(3)	90
Z	8	8	4	4	4	4
V [Å ³]	5383.3(19)	5923.8(4)	3094.79(11)	3119.4(11)	3151.6(9)	3261.1(16)
D_{calc} [g cm ⁻³]	1.403	1.275	1.319	1.351	1.448	1.335
M [mm ⁻¹]	0.104	0.788	0.795	0.101	0.348	0.098
reflns. collected	28489	11924	92947	24251	17609	20148
unique reflns.	7139	3445	7623	4721	6122	4791
observed reflns.	9163	5180	10546	10869	11041	7432
R_1 [$I > 2\sigma(I)$]	0.0407	0.0502	0.0548	0.0486	0.0664	0.0500
wR_2 (all data, F^2)	0.1202	0.1042	0.1587	0.1200	0.1756	0.1316
GOF	1.076	1.013	1.037	0.978	1.097	1.033
largest diff. peak and hole [e·Å ⁻³]	0.447 and -0.228	0.241 and -0.189	0.456 and -0.399	0.319 and -0.288	0.706 and -0.679	0.398 and -0.277

Table 2.

Hydrogen bond parameters of polymorphs and solvated of AM

H-bond	d_{D-H} (Å)	$d_{H...A}$ (Å)	$d_{D...A}$ (Å)	$\angle D-H...A$ (°)	symmetry code
AM-A					
N ₁ -H ₁ ...N ₈	0.91	1.90	2.813(2)	176.0(2)	x, y, z-1
N ₅ -H ₂ ...N ₄	0.86	1.96	2.810(2)	171.1(2)	x, y, z+1
C ₁₀ -H ₁₀ ...O ₁₆	0.93	2.72	3.300(3)	121.8(2)	-x+3/2, y+5/2, -z+3/2
C ₁₆ -H _{16C} ...O ₁₁	0.96	2.57	3.461(3)	154.3(2)	x, y, z-1
C ₁₇ -H _{17A} ...O ₉	0.97	2.52	3.386(2)	148.2(2)	x, y, z-1
C ₂₇ -H _{27C} ...O ₉	0.96	2.50	3.327(3)	144.9(2)	-x+5/2, y+3/2, -z+3/2
C ₃₄ -H ₃₄ ...O ₂	0.93	2.70	3.484(3)	143.2(2)	x+1/2, -y+3/2, z+1/2
C ₄₅ -H _{45A} ...O ₁	0.97	2.47	3.403(2)	161.8(2)	-x+3/2, y+3/2, -z+3/2
C ₄₇ -H _{47A} ...O ₁	0.97	2.67	3.485(3)	142.4(2)	x, y, z+1
AM-B					
N ₁ -H ₁ ...N ₄	0.86	2.04	2.897(3)	175.9(2)	-x+1, y, -z+1/2
C ₄ -H ₄ ...O ₈	0.93	2.64	3.363(4)	134.9(3)	-x+1/2, y+3/2, -z+1/2
C ₆ -H ₆ ...O ₁	0.93	2.44	3.365(4)	170.8(3)	x, y+1, z
C ₂₀ -H _{20B} ...O ₂	0.97	3.33	3.325(4)	132.7(2)	x, y, z
AM-TOL					
N ₁ -H ₁ ...N ₈	0.90	2.01	2.910(3)	174.7(3)	x, y-1, z
N ₅ -H ₂ ...N ₄	0.86	2.00	2.856(3)	171.1(3)	x, y+1, z
C ₁₅ -H _{15B} ...O ₁	0.97	2.46	3.199(3)	132.5(2)	-x+2, -y+1, -z+1
C ₁₇ -H _{17A} ...O ₉	0.97	2.55	3.349(4)	139.2(2)	x, y-1, z
C ₂₃ -H ₂₃ ...O ₁₆	0.93	2.57	3.408(4)	150.0(3)	-x+1, -y+1, -z
C ₂₆ -H _{26A} ...O ₁₆	0.97	2.68	3.403(4)	131.8(3)	x+1, y, z
C ₃₄ -H ₃₄ ...O ₁₆	0.93	2.47	3.321(4)	152.5(3)	x+1, y, z
C ₅₉ -H _{59C} ...O ₈	0.96	2.59	3.487(5)	155.3(3)	-x+1, -y+1, -z
AM-DIO					
N ₁ -H ₁ ...N ₈	0.93	1.88	2.802(4)	170.2(4)	x, y, z
N ₅ -H ₂ ...N ₄	0.89	1.96	2.845(4)	176.5(3)	x, y, z
C ₄ -H ₄ ...O ₁	0.93	2.58	3.373(6)	143.8(3)	-x, -y, -z+1
C ₆ -H ₆ ...O ₁₄	0.93	2.56	3.429(6)	156.5(4)	-x+1, -y+1, -z+1
C ₁₇ -H _{17B} ...O ₉	0.97	2.55	3.326(4)	137.3(3)	x, y, z
C ₂₇ -H _{27A} ...O ₁₆	0.96	2.26	3.209(5)	170.6(3)	x, y-1, z
C ₃₅ -H ₃₅ ...O ₉	0.93	2.68	3.493(5)	146.5(4)	-x+1, -y+1, z
C ₃₇ -H ₃₇ ...O ₁₉	0.93	2.55	3.455(3)	164.1(3)	x, y, z
C ₄₁ -H ₄₁ ...O ₉	0.93	2.64	3.452(4)	146.0(3)	-x, -y+1, -z
C ₄₆ -H _{46B} ...O ₈	0.96	2.59	3.476(5)	153.0(3)	x, y, z
C ₆₀ -H _{60C} ...O ₈	0.96	2.51	3.364(5)	149.0(4)	x-1, y+1, z
C ₆₀ -H _{60B} ...O ₉	0.96	2.54	3.490(5)	169.5(4)	-x, -y+1, -z
C ₆₂ -H _{62B} ...O ₁	0.97	2.68	3.298(7)	122.3(6)	x+1, y, z

AM-TCM					
$N_1-H_1\cdots N_8$	0.86	2.02	2.882(5)	173.0(4)	x, y, z
$N_5-H_2\cdots N_4$	0.81	2.06	2.864(5)	176.5(4)	x, y, z
$C_6-H_6\cdots O_8$	0.93	2.57	3.248(6)	129.7(4)	-x+1, y, -z+2
$C_{17}-H_{17B}\cdots O_9$	0.97	2.53	3.330(5)	139.5(4)	x, y, z
$C_{26}-H_{26A}\cdots O_{16}$	0.97	2.50	3.215(6)	130.7(4)	x-1, y-1, z
$C_{34}-H_{34}\cdots O_{16}$	0.93	2.48	3.371(6)	159.3(4)	x-1, y, z
$C_{48}-H_{48B}\cdots O_1$	0.97	2.43	3.180(6)	134.3(7)	x, y, z
$C_{54}-H_{54}\cdots O_9$	0.93	2.71	3.469(6)	138.9(4)	x+1, y, z
AM-DMA					
$N_1-H_1\cdots O_9$	0.88	1.86	2.744(2)	177.1(2)	x, y, z
$C_{15}-H_{15A}\cdots O_1$	0.97	2.34	3.183(3)	145.0(2)	-x+1/2, y+3/2, -z+5/2
$C_{21}-H_{21}\cdots O_9$	0.93	2.54	3.389(3)	152.1(2)	x-1/2, -y+1/2, z-1/2
$C_{31}-H_{31B}\cdots O_1$	0.96	2.64	3.425(4)	139.4(2)	-x+1/2, y+3/2, -z+5/2

Table 3. $\pi \cdots \pi$ or C-H $\cdots\pi$ interactions in polymorphs and solvates of AM

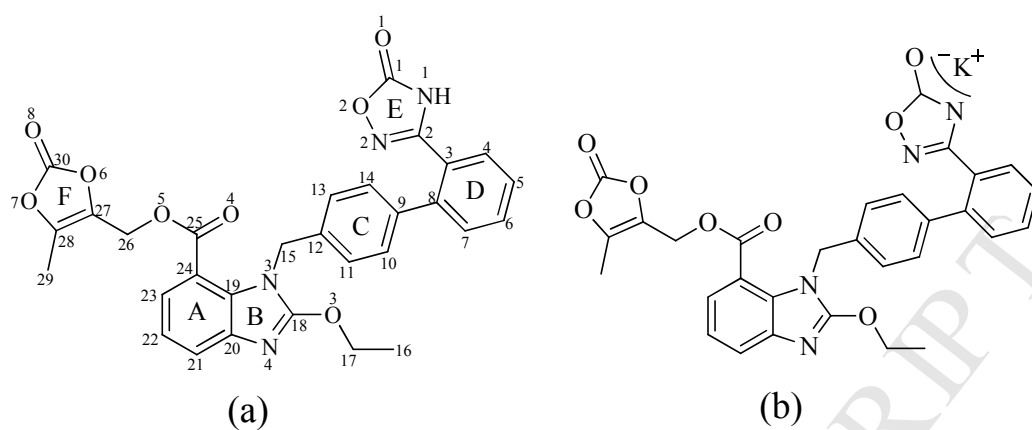
Compound	Interaction ^a	R (Å) ^b	Angle (°)
AM-A	$\pi_{B2} \cdots \pi_{B2}$	3.980(2)	0
	$C_{17}-H_{17B} \cdots \pi_{C2}$	3.623(2)	159.6(3)
	$C_{21}-H_{21} \cdots \pi_{D2}$	3.986(2)	130.5(2)
	$C_{47}-H_{47B} \cdots \pi_{C1}$	3.677(2)	156.3(2)
	$C_{51}-H_{51} \cdots \pi_{D1}$	3.849(2)	118.9(2)
	$C_{53}-H_{53} \cdots \pi_{A1}$	3.674(2)	137.1(2)
AM-B	$\pi_A \cdots \pi_B$	3.806(3)	0
	$C_{25}-H_{25} \cdots \pi_D$	3.501(3)	139.1(2)
	$C_{30}-H_{30A} \cdots \pi_C$	3.774(3)	158.2(2)
AM-DIO	$C_{27}-H_{27C} \cdots \pi_{D2}$	3.561(4)	148.1(4)
	$C_{47}-H_{47B} \cdots \pi_{C1}$	3.809(4)	161.9(4)
	$C_{63}-H_{63B} \cdots \pi_{A1}$	4.394(4)	152.3(4)
AM-DMA	$C_{33}-H_{33C} \cdots \pi_D$	3.731(3)	148.0(2)
	$C_{34}-H_{34A} \cdots \pi_D$	3.987(3)	128.9(2)

^a π is defined as the centroid of the ring.^b R is defined as the distance between the centroids of the rings.

Table 4.

Dihedral angles (°) in polymorphs and solvates of AM

Compounds	A-B	A-C	C-D	D-E
AM-A	1.1(3)	86.4(3)	44.2(2)	51.4(3)
	1.7(3)	89.7(3)	47.3(2)	61.3(3)
AM-B	3.5(3)	73.4(3)	51.5(2)	60.6(2)
AM-TOL	3.2(3)	83.6(3)	45.9(3)	58.5(3)
	5.2(3)	69.6(3)	50.6(3)	58.6(3)
AM-DIO	0.5(4)	80.1(4)	48.5(4)	49.3(2)
	0.7(4)	87.1(4)	41.7(4)	58.2(2)
AM-TCM	2.1(4)	87.9(4)	50.0(4)	59.0(3)
	3.0(4)	77.2(4)	49.0(4)	62.5(3)
AM-DMA	0.2(2)	82.0(3)	40.5(2)	56.2(2)



Scheme 1. Chemical structures of azilsartan medoxomil (a) and azilsartan medoxomil potassium (b). Digits and letters are the atomic codes and ring codes.

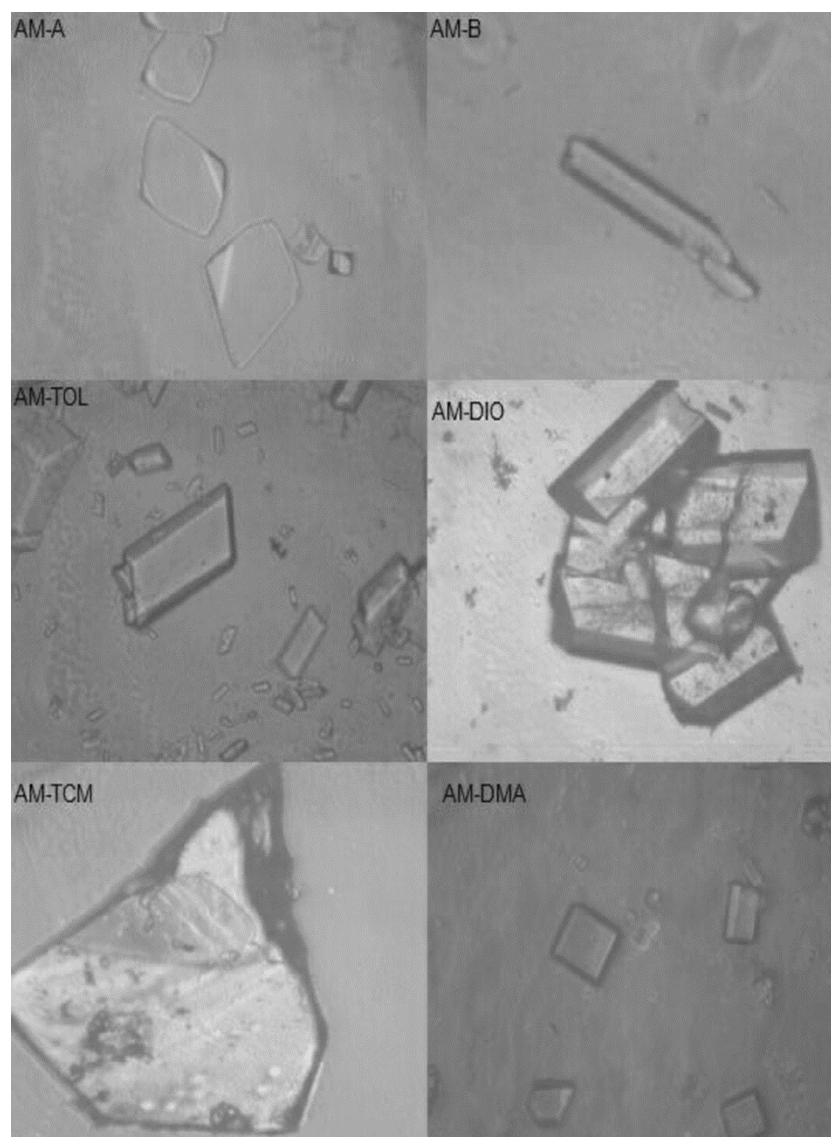


Fig. 1. Photographs of crystals for polymorphs and solvates of AM ($\times 100$).

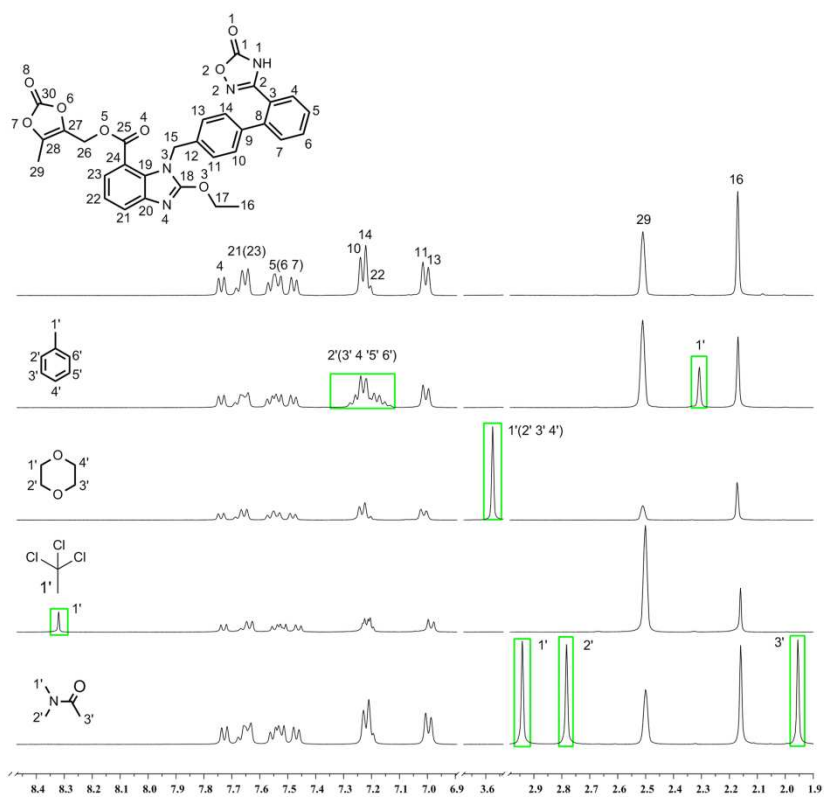


Fig. 2. $^1\text{H-NMR}$ spectra for AM-A, AM-TOL, AM-DIO, AM-TCM and AM-DMA.

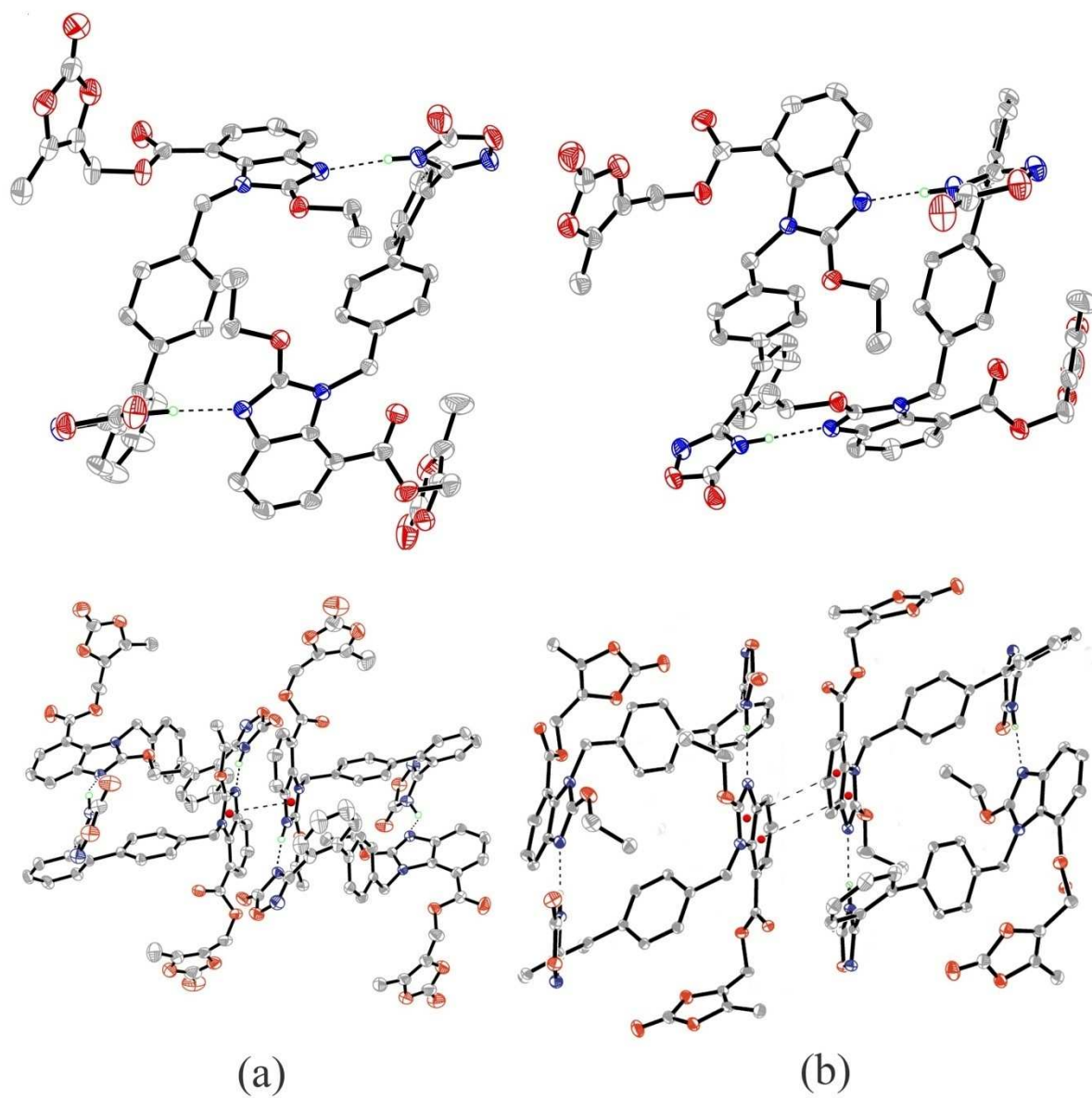


Fig. 3. The crystal structures and interactions of polymorphs AM-A (a) and AM-B (b).

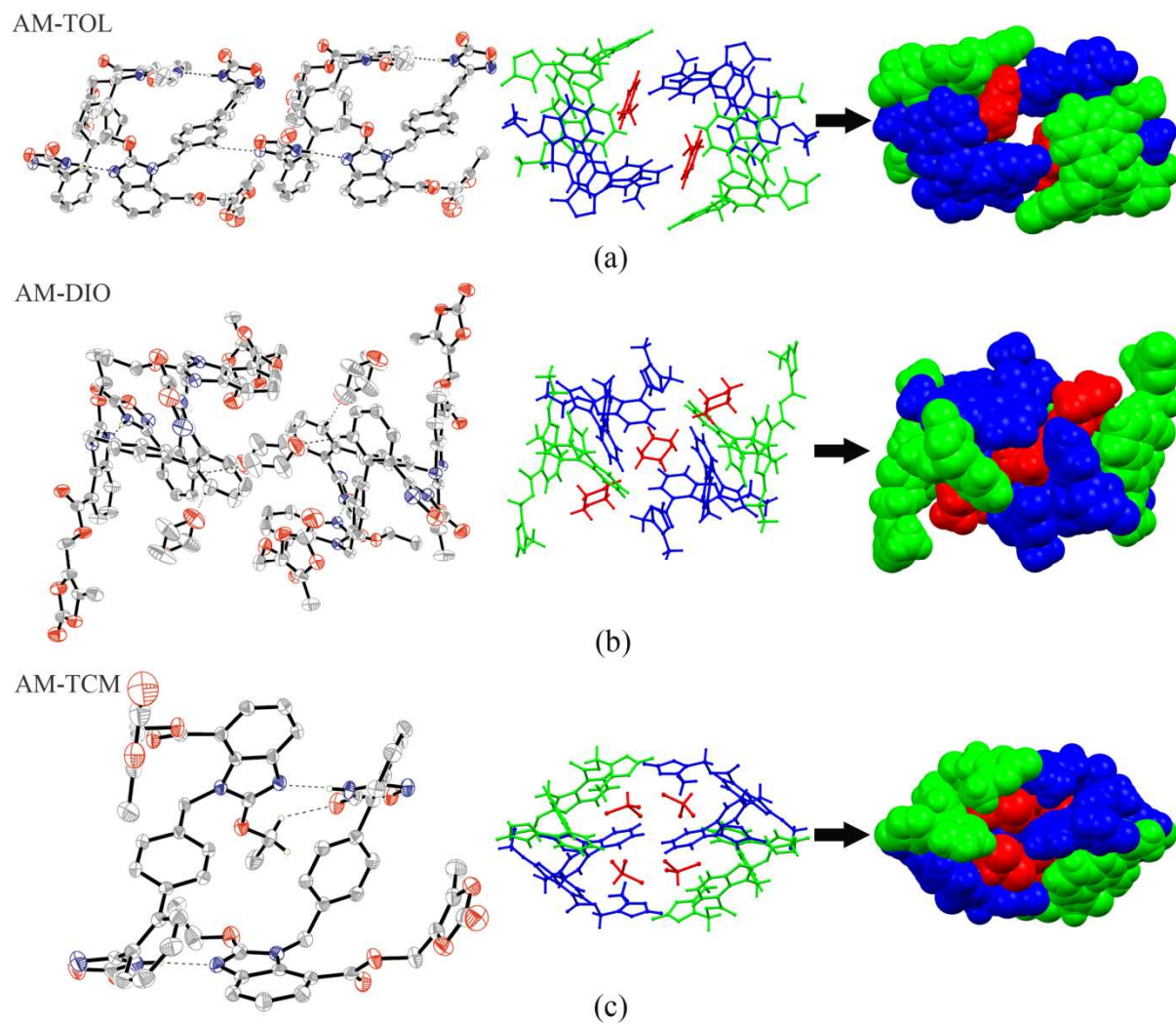


Fig. 4. Illustration for the crystal structures of AM-TOL (a), AM-DIO (b) and AM-TCM (c).

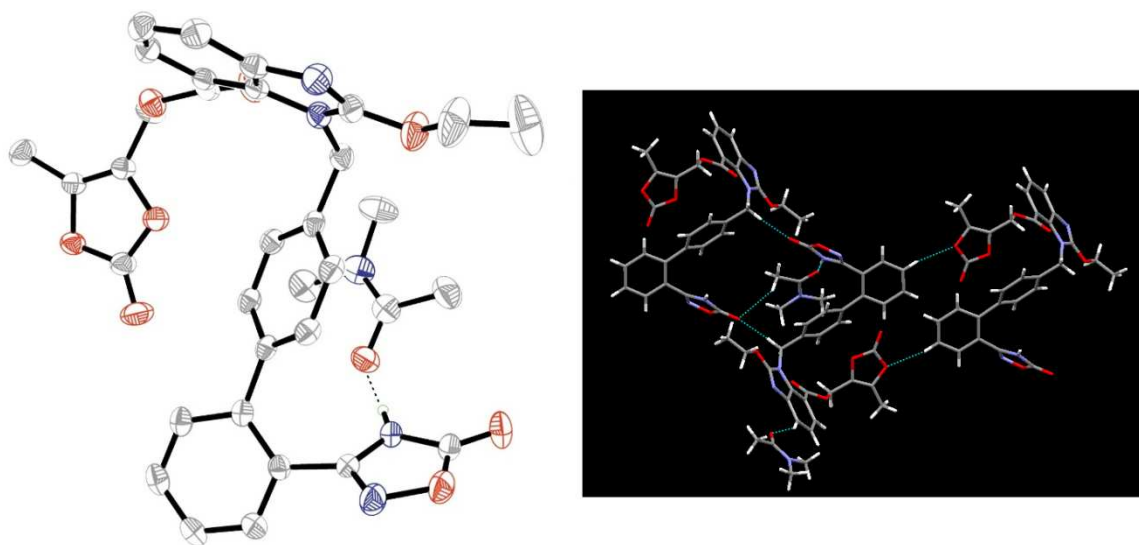


Fig. 5. The crystal structure and hydrogen bond interactions of AM-DMA.

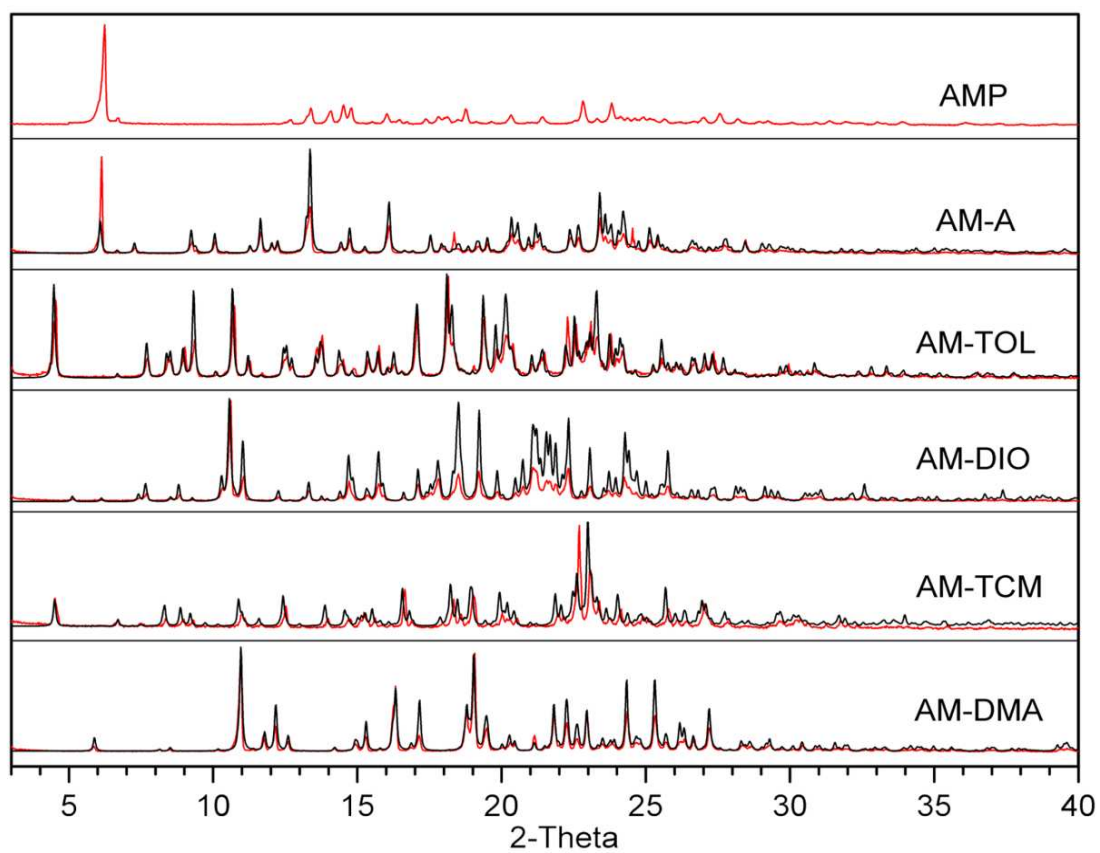


Fig. 6. Experimental (red) and simulated (black) PXRD patterns for AMP, AM-A and four solvates.

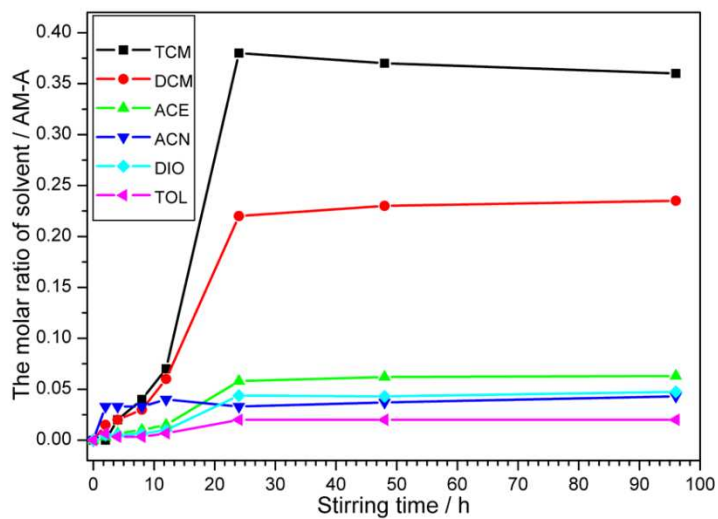


Fig. 7. The amount of inclusion solvent per AM molecule upon soaking time.

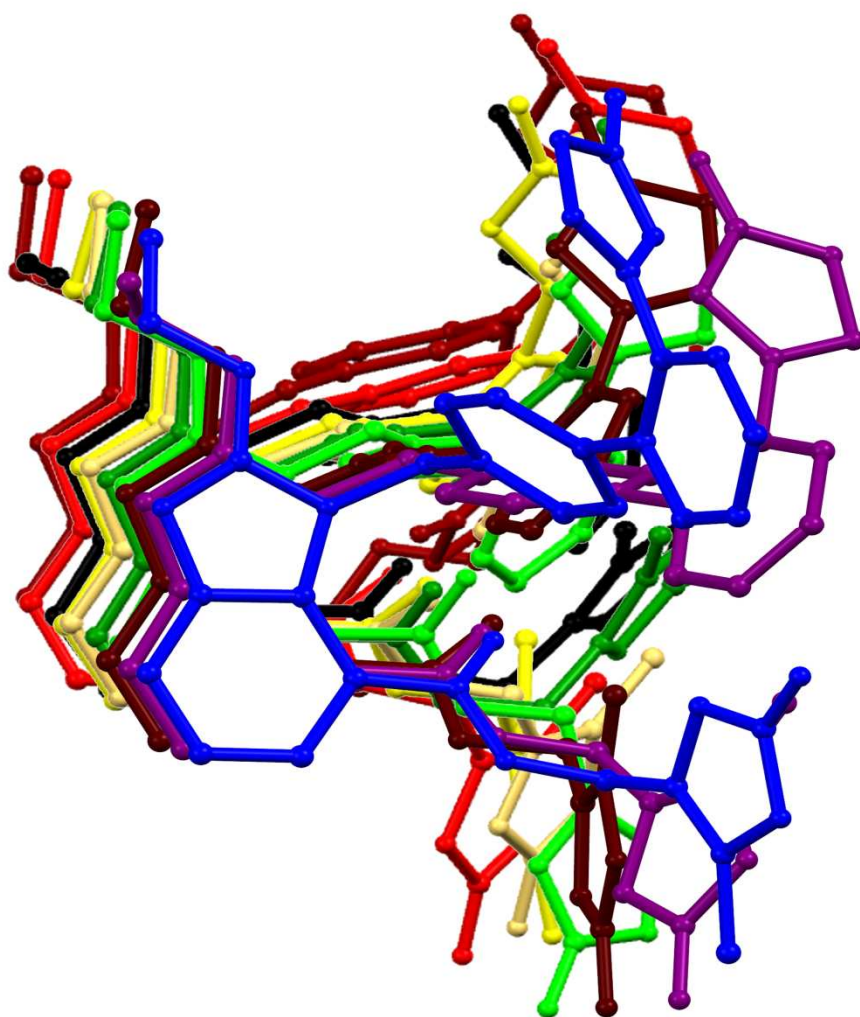


Fig. 8. Overlay diagram of ten AM conformers in different crystal structures drawn by fixing the benzimidazolyl plane.

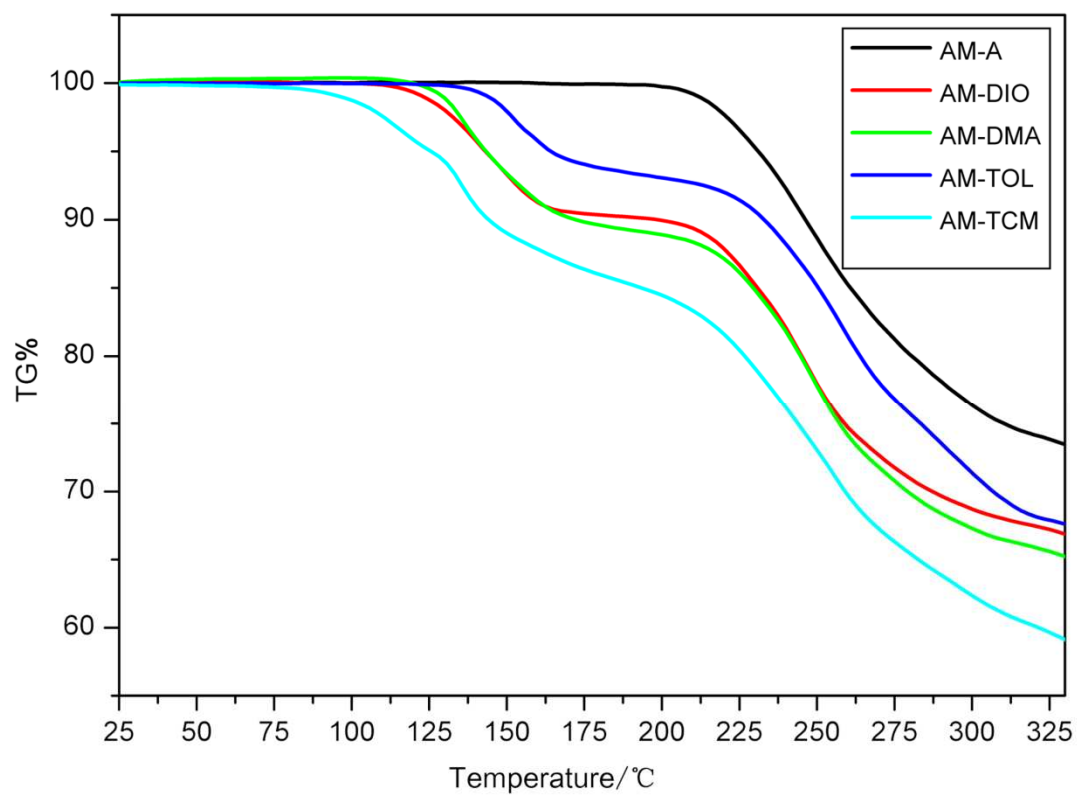


Fig. 9. TGA curves of AM-A and four solvates.

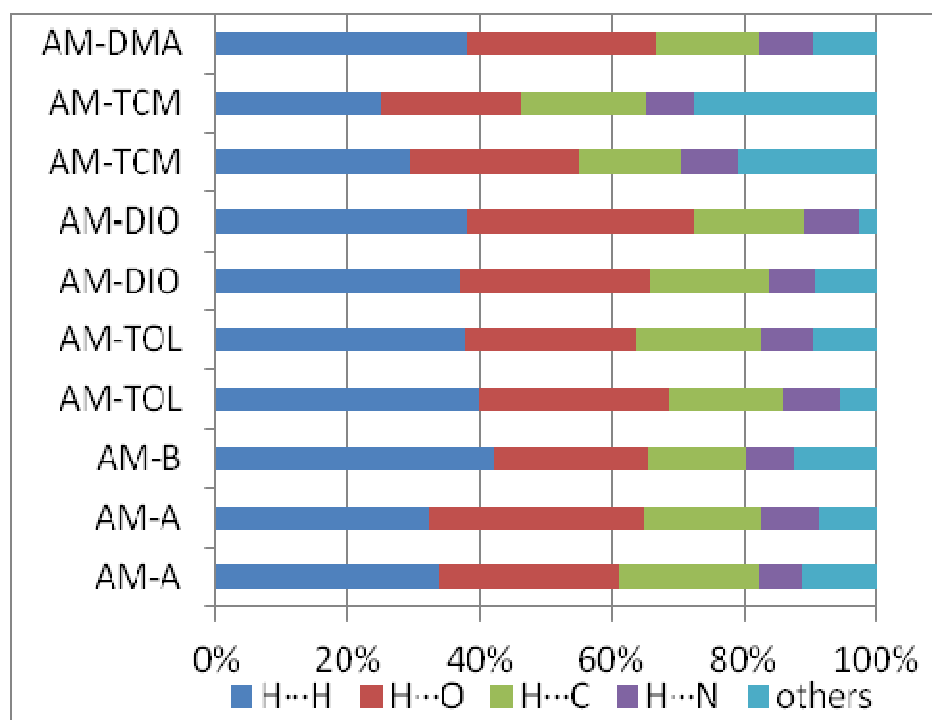


Fig. 10. Percentage distribution of individual intermolecular interactions on the basis of Hirshfeld surface analysis of ten AM conformers in different crystal structures.